

# Modeling Electrical and Thermal Conductivities of Biological Tissue in Radiofrequency Ablation

M. Trujillo<sup>\*1</sup>, E. Berjano<sup>2</sup>

<sup>1</sup>Instituto Universitario de Matemática Pura y Aplicada, Universitat Politècnica de València, Spain and <sup>2</sup>Biomedical Synergy, Electronic Engineering Department, Universitat Politècnica de València, Spain

\*Corresponding author: Camino de Vera. 46022. Valencia. Spain, [matrugui@mat.upv.es](mailto:matrugui@mat.upv.es)

**Abstract:** Radiofrequency ablation (RFA) is a minimally invasive technique used to treat some kinds of cancer. Theoretical models can provide information about the biophysics of RFA quickly and cheaply, but their realism is very important. A great influential factor in this realism is the use of mathematical functions to model the temperature-dependence of tissue thermal ( $k$ ) and electrical ( $\sigma$ ) conductivities. The aim of this work is to review the mathematical functions employed to model temperature-dependence of  $k$  and  $\sigma$  in previous RFA computer modeling studies and to assess how these different functions affect lesion dimension evolution. We use a model of RF hepatic ablation in which both conductivities are modeled with different mathematical functions and compare the lesion sizes obtained in every case. We solve numerically the problem using COMSOL Multiphysics. Results suggest that the different functions to model the temperature dependence of  $k$  and  $\sigma$  do not significantly affect the computed lesion diameter.

**Keywords:** Radiofrequency ablation, electrical conductivity, thermal conductivity.

## 1. Introduction

Radiofrequency ablation (RFA) is a minimally invasive technique used to treat some kinds of cancer [1], [2]. In RFA electrical currents ( $\approx 500$  kHz) are employed to heat the target biological tissue over  $50^\circ\text{C}$ . Theoretical modeling is a usual method to study the biophysics of RFA. However, it is necessary that models are realistic to obtain meaningful results. The mathematical functions used to model the temperature-dependence of electrical ( $\sigma$ ) and thermal ( $k$ ) conductivities are one of the most important factors which influence the realism. At the literature we found different ways to model this dependence. The question was: The use of different mathematical functions to model the

temperature dependence of  $\sigma$  and  $k$  produce great variations in results? Our objective was to answer this question. We focused our attention in piecewise functions employed for this task. We considered 32 cases in which  $\sigma$  and  $k$  are represented with different mathematical functions. To achieve our objective we used a radiofrequency hepatic model which varied depending on the function employed to model  $\sigma$  and  $k$ . We solved the model using COMSOL Multiphysics software (COMSOL, Burlington MA, USA). We contrasted the results of every case using the lesion size as a parameter of comparison.

## 2. Functions to model temperature-dependence of electrical and thermal conductivities

We focused our attention in the most usual piecewise mathematical functions employed to model the temperature dependence of  $\sigma$  and  $k$ .

### 2.1 Electrical conductivity, $\sigma$

Electrical conductivity increases with temperature up to  $100^\circ\text{C}$ . After this temperature  $\sigma$  drops abruptly. The most usual piecewise functions we found at the literature [3]-[7] can be summarized as follows:

- 1) For temperatures below  $100^\circ\text{C}$ , two increase rates: 1.5 and  $2\%/^\circ\text{C}$ , and two increase types: linear and exponential.
- 2) For temperatures above  $100^\circ\text{C}$ , two drop rates: 2 and 4 orders of magnitude between  $100^\circ\text{C}$  and  $105^\circ\text{C}$ .

These combinations of  $\sigma$  allowed up to 8 cases (see Table 1).

### 2.2 Thermal conductivity, $k$

It is known that thermal conductivity is a

**Table 1.** Studied cases according to the different mathematical functions used to model the temperature dependence of electrical ( $\sigma$ ) conductivity.

$\sigma$ cases	T<100°C				T>100°C	
	Linear growth (%/°C)		Exponential growth (%/°C)		$\sigma$ drops rate 2 orders	$\sigma$ drops rate 4 orders
	1.5	2	1.5	2		
1	X				X	
2		X			X	
3			X		X	
4				X	X	
5	X					X
6		X				X
7			X			X
8				X		X

temperature-dependent parameter. However, we have found that in the most of the models  $k$  is assumed to be constant [6]. In cases in which  $k$  is described as a mathematical piecewise functions can be summarized as follows:

- 1) A linear increase rate of 1.5%/°C for temperatures below 100°C, and a constant value for temperatures above 100°C [5].
- 2) A different value before and after water vaporization, i.e. a different value for each phase, liquid and gas [8].
- 3) A linear drop rate of -1.5%/°C for temperatures below 100°C, and a constant value for temperatures above 100°C [9].

In this work we compared the results of a RFA model taking into account these mathematical functions and a constant value of  $k$ .

### 3. RFA modeling with COMSOL Multiphysics

To compare the effect of the different combinations of the mathematical functions presented in the previous section, we considered a theoretical radiofrequency hepatic ablation model which consisted of a fragment of hepatic tissue and an internally cooled electrode. The model was based on a coupled electric-thermal problem, which was solved numerically using COMSOL Multiphysics software (COMSOL,

Burlington MA, USA). The problem presented axial symmetry and hence a two-dimensional analysis was conducted (see Figure 1 to see the problem geometry). We chose in the model navigator of COMSOL a 2D problem with axial symmetry. For the physics we use a Multiphysics model with a Conductive Media DC and Bioheat Equation (transient analysis) as application modes.

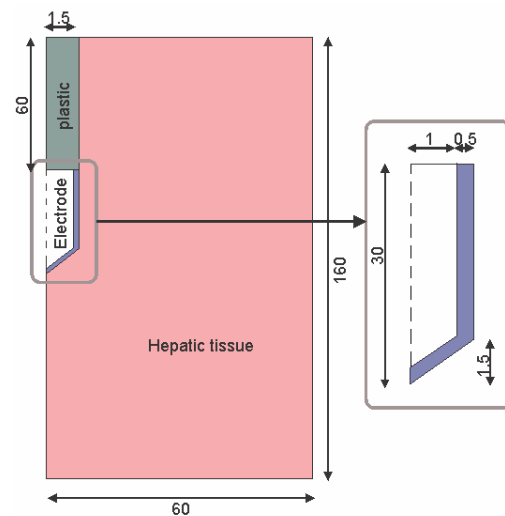


**Figure 1.** Geometry of the model, out of scale. Dimensions in mm.

The most of the model parameters were inserted in COMSOL using Constants option [7,10,11,12]. We used Expressions option for inserting the mathematical functions which represent  $\sigma$  and  $k$ . We conducted a set of 32 simulations including all cases considered in sections 2.1 and 2.2 in order to assess the effect of  $\sigma$  and  $k$ .

The bioheat equation was used as the governing equation of the thermal problem. The enthalpy method was considered to modify the bioheat equation and hence to incorporate the phase change [8]. The metabolic heat is negligible in this kind of problems. The blood perfusion term  $Q_p$  was obtained from

$$Q_p = \beta \rho_b c_b \omega_b (T_b - T) \quad (1)$$

where  $\rho_b$  is density of blood [6],  $c_b$  specific heat of blood [3],  $T_b$  blood temperature  $\omega_b$  blood perfusion coefficient [13] and  $\beta$  is a coefficient which took the values of 0 and 1, depending on the value of the local thermal damage  $\Omega$ :  $\beta = 0$

for  $\Omega \geq 1$ , and  $\beta=1$  for  $\Omega < 1$ . The parameter  $\Omega$  was assessed by the Arrhenius damage model [13]. We employed the thermal damage contour D63 to compute the lesion dimension contour, which corresponds to  $\Omega=1$  (63% probability of cell death). The heat source from RF power  $q$  (Joule losses) was given by  $q=\sigma|\mathbf{E}|^2$ , where  $\mathbf{E}$  is an electric field which was obtained from the electrical problem. The Laplace equation  $\nabla^2 V=0$  was the governing equation for the electric problem,  $V$  being the voltage. The electric field was calculated by means of  $\mathbf{E} = -\nabla V$ . We used a quasi-static approach, i.e. tissues were considered as purely resistive due to the value of the frequencies used in RF ( $\approx 500$  kHz) and for the geometric area of interest (electrical power is deposited in a very small zone close to the electrode).

Thermal boundary conditions were: Null thermal flux in the transversal direction to the symmetry axis. Constant temperature of  $37^\circ\text{C}$  in the dispersive electrode (lower geometry contour). Initial temperature of the tissue was considered to be  $37^\circ\text{C}$ . The cooling effect produced by the liquid circulating inside the electrode was modeled using a thermal convection coefficient  $h$  with a value of  $3366 \text{ W/K}\cdot\text{m}^2$  and a coolant temperature of  $10^\circ\text{C}$  following the Newton's law of cooling.

Electrical boundary conditions were: Zero current density in the transverse direction to the symmetry axis and inside the electrode and zero voltage in the dispersive electrode. The delivery of the energy followed a pulsed RF protocol controlled by the roll-off time, roll-off being the time at which tissue impedance is  $30 \Omega$  higher than the initial.

This procedure, common in clinical practice, is repeated for a period of 6-12 min. The simulations lasted for up to 6 minutes and the protocol was implemented by means of a connection between COMSOL and Matlab (MathWorks, Natick, MA, USA).

The model mesh was heterogeneous, with a finer mesh size at the electrode-tissue interface, where the highest electrical and thermal gradients were expected. All the mesh elements used were triangular. In the case of the time-step we used an adaptive scheme since we let the time-stepping method chose time steps freely.

#### 4. Results

We obtained the lesion size evolution for the 32 cases considered. More specifically, we are interested in the value of the lesion short diameter  $a$  (transverse diameter). Firstly, we compared lesion sizes varying  $\sigma$  according to the different mathematical functions considered in section 2.1 (see Table 1) and  $k$  represented always with the same function. Figure 2 shows the evolution of the lesion short diameter throughout 360 s for cases 1 to 4 with  $k$  as a constant. Dashed lines represent the time in which the first roll-off was achieved in each case. The maximum difference was 6% between cases 1 and 4 at  $\approx 220$  s. This difference was only 3.5% at 6 minutes. The same comparison was made for cases 5 to 8 (not shown) and differences in the lesion short diameter were always smaller. We also obtained the evolution of the lesion short diameter for cases 1-8 but varying  $k$  according the mathematical functions considered in section 2.2. Differences are negligible between all the cases considered for  $k$ .

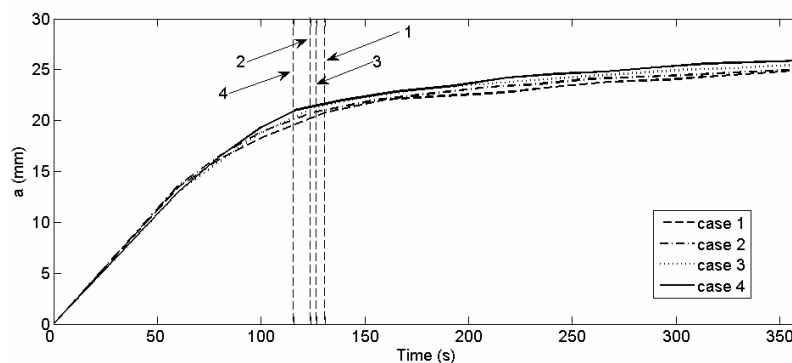


**Figure 2.** Evolution of the lesion short diameter ( $a$ ) throughout 360 s for cases 1 to 4 (see Table 1 for details). Dashed lines represent the time in which the first roll-off was achieved in each case.

## 5. Discussion

We have noticed that differences in lesion size between all cases considered for  $\sigma$  were small ( $< 6\%$ ). However, differences for cases in which  $k$  varies were still smaller, negligible in fact. This finding supports that in RFA modeling is usual to use a constant value of  $k$  without loss of realism.

One of the limitations of this study is that we focused on piecewise mathematical functions as they are the most commonly used. However, it must be said that other kinds of mathematical functions can be used to model these characteristics in RFA. Pearce et al. [14] considered water as the most thermodynamically active tissue constituent and both their formulation and the functions used to model  $\sigma$  and  $k$  take into account the tissue water content. As regards  $\sigma$ , some studies have considered a temperature-dependence based on a polynomial relation derived from NaCl solutions [15,16]. Ji and Brace [17] recently have suggested that variations in liver electrical conductivity at temperatures near  $100^\circ\text{C}$  are best modeled using a sigmoid function for microwave thermal ablation.

Our aim was not to choose the most suitable function to represent the temperature-dependence of  $\sigma$  and  $k$ , which would need additional experimental studies outside the scope of this work.

## 6. Conclusion

In RFA the temperature dependence of  $\sigma$  below  $100^\circ\text{C}$  can be modeled equally well either by using a linear or exponential increase or an increase rate of between  $+1.5\%/^\circ\text{C}$  and  $+2\%/^\circ\text{C}$  and above  $100^\circ\text{C}$  can be modeled equally well by using an abrupt drop of either 2 or 4 orders of magnitude between  $100^\circ\text{C}$  and  $105^\circ\text{C}$ . In the context of this study, the term “equally” means that the computed lesion short diameter after 6 minutes ablation differs by less than  $3.5\%$ . The temperature dependence of  $k$  can be ignored and hence a constant value can be used.

## 7. References

1. Benoist S, Nordlinger B, Radiofrequency ablation in liver tumors, *Ann Oncol* **15**, 313–7 (2004).
2. Sharma R, Wagner JL, Hwang RF, Ablative therapies of the breast, *Surg Oncol Clin N Am*, **20**:317–39 (2011).
3. Tungjitkusolmun S, Woo EJ, Cao H, Tsai JZ, Vorperian VR, Webster JG, Thermal-electrical finite element modeling for radio frequency cardiac ablation: effects of changes in myocardial properties, *Med Biol Eng Comput*, **38**, 562–8 (2008).
4. Dodde RE, Miller SF, Geiger JD, Shih AJ, Thermal-electric finite element analysis and experimental validation of bipolar electrosurgical cautery, *J Manuf Sci Eng*, **130**, 1-8 (2008).
5. Byeongman J, Aksan A, Prediction of the extent of thermal damage in the cornea during conductive thermokeratoplasty, *J Therm Biol*, **35**, 167–74 (2010).
6. Haemmerich D, Chachati L, Wright AS, Mahvi DM, Lee FT, Webster JG, Hepatic radiofrequency ablation with internally cooled probes: effect of coolant temperature on lesion size, *IEEE Trans Biomed Eng*, **50**, 493–9 (2003).
7. Pätz T, Kröger T, Preusser T, Simulation of radiofrequency ablation including water evaporation. *IFMBE Proceedings*, **25/IV**, 1287–90 (2009).
8. Abraham JP, Sparrow EM, A thermal-ablation bioheat model including liquid-to-vapor phase change, pressure- and necrosis-dependent perfusion, and moisture-dependent properties. *Int J Heat Mass Transfer*, **50**, 2537–44 (2007).
9. Baldwin SA, Pelman A, Bert JL, A heat transfer model of thermal balloon endometrial ablation, *Ann Biomed Eng*, **29**, 1009–18 (2001).
10. Duck F, Physical properties of tissue-A comprehensive reference book. *Academic Press*, New York (1990).
11. Berjano EJ, Burdío F, Navarro AC, Burdío JM, Güemes A, Aldana O, et al, Improved perfusion system for bipolar radiofrequency ablation of liver: preliminary findings from a computer modeling study. *Physiol Meas* **27**, N55–66 (2006).
12. Trujillo M, Alba J, Berjano E, Relation between roll-off occurrence and spatial distribution of dehydrated tissue during RF ablation with cooled electrodes, *Int J Hyperthermia*, **28**, 62–8 (2012).
13. Chang IA, Considerations for thermal injury analysis for RF ablation devices, *Biomed Eng Online*, **4**, 3-12 (2010).

14. Pearce J, Panescu D, Thomsen S, Simulation of diopter changes in radio frequency conductive keratoplasty in the cornea, *WIT Trans Biomed Health*, **8**, 469–77 (2005).
15. Chang IA, Nguyen UD, Thermal modeling of lesion growth with radiofrequency ablation devices, *Biomed Eng Online* 2004;3:27.
16. Barauskas R, Gulbinas A, Barauskas G, Investigation of radiofrequency ablation process in liver tissue by finite element modeling and experiment, *Medicina (Kaunas)*, **43**, 310–25 (2007).
17. Ji Z, Brace CL, Expanded modeling of temperature-dependent dielectric properties for microwave thermal ablation, *Phys Med Biol*, **56**, 5249–64 (2011).

## 9. Acknowledgements

This work received financial support from the Spanish “Plan Nacional de I+D+I del Ministerio de Ciencia e Innovación” grant No. TEC2011-27133-C02-01 and from the PAID-06-11 UPV grant Ref. 1988.